Synthesis, structure and magnetic properties of an oxamate-based 1D coordination polymer built on pentametallic links

Ang Li, Jérémy Forté, Yanling Li, Yves Journaux, Laurent Lisnard

Synthesis, structure and magnetic properties of an oxamate-based 1D coordination polymer built on pentametallic links.

Ang Li (李昂),[a] Jérémy Forté,[a] Yanling Li,[a] Yves Journaux,[a] Laurent Lisnard*[a]

a. Sorbonne Université, CNRS, Institut Parisien de Chimie Moléculaire, IPCM, F-75252, Paris, France.

*Corresponding author: laurent.lisnard@sorbonne-universite.fr

Abstract

The solvothermal reaction of the hexadentate 2-(oxamato)benzoic acid ligand (oaba) with copper(II) and cobalt(II) ions has yielded the $[Cu_4Co_3(oaba)_4(OH)_2(DMF)_6]\cdot 2(DMF)\cdot 1H_2O$ (**1**) 1D coordination polymer. The single-crystal X-ray diffraction study reveals the formation of a neutral chain built from pentametallic complexes where each multi-polydentate ligand bridges four metal centres. The atypical morphology observed here for an oxamate-based 1D polymer arises from the use of a ligand bearing extra coordination sites. Magnetometry indicates strong dominating antiferromagnetic interactions within the polymer resulting in a non-zero ferrimagnetic state at low temperature.

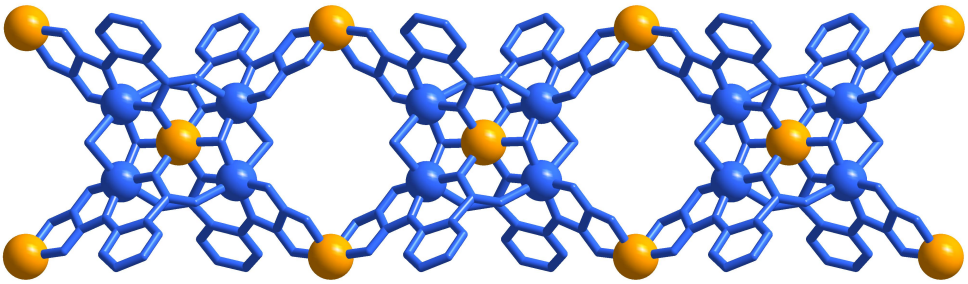

Keywords

Oxamate ligand; multi-polydentate ligand; solvothermal synthesis; coordination polymer; heterobimetallic compound.

1. Introduction

Oxamate ligands are attractive synthetic tools with a rich coordination chemistry that facilitates the design and preparation of molecular materials.[1–7] While phenyl-based oxamate ligands,[8–11] and amino-acid-based oxamate ligands now represent the bulk of the investigations,[12–23] a sub-class of aromatic oxamate ligands that are substituted with additional –non-oxamic– coordinating groups starts to gain attention.[24–33] Like the amino-acid-based oxamate ligands, such *multi*-polydentate ligands bearing additional carboxylato, hydroxido or N-donor groups offer diverse coordination modes with metal ions, which give access to new structural types. Recently, this led us to investigate the reactivity of the 2-hydroyphenyloxamate ligand and we have observed the formation of two atypical structures for phenyloxamate-related chemistry: a hexametallic macrocyclic coordination ring and of a chiral coordination polymer.[34] To further this reactivity investigation, we have also decided to revisit solvothermal reactions. Indeed, prior attempts by others and us at using this technique for reacting oxamate ligands highlighted difficulties in obtaining a fully deprotonated, i.e. fully coordinating, form of the oxamate ligand.[32,35] Nevertheless, the use of solvothermal reactions for the 2-hydroyphenyloxamate ligand was successful, and we were able to isolate a 1D coordination polymer.[36] To continue our study, we have extended the use of solvothermal conditions to the ortho-substitued carboxylatophenyloxamate ligand (2-(ethyloxamate)benzoic acid, H_2Et-oaba) in the presence of copper(II) and cobalt(II) ions. It has resulted in the formation of a novel 1D coordination polymer, $[Cu_4Co_3(oaba)_4(OH)_2(DMF)_6]\cdot 2(DMF)\cdot 1H_2O$, (**1**), where the hexadentate ligand generates pentametallic building blocks. We present here the synthesis, structural and magnetic characterizations of **1**.

2. Experimantal section

2.1. Materials and methods

All reagents were used as purchased with no further purification. The ester proligand 2-(ethyloxamate)benzoic acid (H_2Et-oaba) was prepared here according to the general procedure for oxamate ligand,[37] which differs from the previously reported synthesis for H_2Et-oaba.[25] Elemental analysis was performed in the “service de microanalyse” at ICSN (CNRS, Gif/Yvette, France) and via the PARI program at the IPGP (Paris, France). ATR/FT-IR spectra were collected on a Bruker TENSOR 27 equipped with a simple reflexion ATR diamond plate of the Harrick MPV2 series. The thermogravimetric analysis (TGA) was performed on a TA Instruments SDTQ600 under air or nitrogen with a heating rate of 5 °C/min. ^{1}H and ^{13}C NMR spectra were collected on 300 and 400 MHz Bruker Avance spectrometers at 298 K.

2.2. Synthesis

2.2.1. Ligand preparation, ester proligand: 2-(ethyloxamate)benzoic acid, H_2Et-oaba.

To 6.0 g of anthranilic acid (M=137.14 gmol^{-1}, 43.75 mmol) in 250 mL of THF were added dropwise 5.5 mL of ethyloxalyl chloride (98%; 1eq.) under strong stirring. The mixture was refluxed for 120 min and filtered on paper while hot (some white residue is filtered off). Removal of the solvent under reduced pressure yields a white powder. The powder was washed with 700 mL of water under stirring for 30 min and then collected on a sintered glass filter. Further washing was done with cold 50 % ethanol and the solid was dried in air. The final product was collected as a white powder (9.15 g, Yield: 88.17 %, M=237.2 gmol^{-1}). ^{1}H-NMR (400 MHz, DMSO) δ (ppm): 12.56 (s, 1H), 8.57 (d, *J* = 8.4 Hz, 1H), 8.02 (d, *J* = 7.9 Hz, 1H), 7.67 (t, *J* = 8.6 Hz, 1H), 7.26 (t, *J* = 8.6 Hz, 1H), 4.29 (q, *J* = 7.1 Hz, 2H), 1.30 (t, *J* = 7.1 Hz, 3H). ^{13}C-NMR (75 MHz, DMSO) δ (ppm): 169.20 (s, -COO-), 159.76 (s, -COO-), 154.32 (s, -CONH-), 139.27 (s, -PhNH-), 134.34 (s, Ph), 131.37 (s, Ph), 123.98 (s, Ph), 119.56 (s, Ph), 116.90 (s, PhCOOH), 62.82 (s, -CH_2-), 13.74 (s, -CH_3). FTIR (cm-1): 3501 (m), 3416 (m), 2982 (w), 2481 (w), 1755 (s), 1689 (s), 1663 (s), 1589 (m), 1519 (s), 1466 (m), 1452 (w), 1428 (w), 1297 (m), 1248 (s), 1188 (s), 1092 (w), 999 (m), 929 (w), 858 (m), 822 (w), 789 (s), 762 (s), 698 (m), 660 (m), 602 (m), 510 (m), 356 (m), 320 (m), 275 (m). Elemental analysis (%): calc. for $C_{11}H_{11}NO_5$. C, 55.70; H, 4.67; N, 5.90 Found: C, 55.46; H, 4.59; N, 5.96.

2.2.2. Ligand preparation, acid form: 2-(oxamato)benzoic acid hydrate, mixed sodium salt, $H_{2.5}Na_{0.5}$-oaba·0.5(H_2O).

To 2.7 g of H_2Et-oaba (M = 237.2 gmol^{-1}; 11.38 mmol) suspended in 300 mL of water were slowly added 11.3 mL of 2M NaOH (2eq). The solution was stirred for 30 min and filtered on paper. Under stirring, 5.7 mL of 4M HCl (3eq.) were added dropwise and a precipitate formed gradually. The stirring was maintained for another 30 min and the solid was collected on a sintered glass filter, and dried in an oven at 70 °C overnight. (2.34 g, Yield: 89.75 %, M= 229.1 gmol^{-1}). ^{1}H-NMR (400 MHz, DMSO) δ (ppm): 12.53 (s, 1H), 8.65 (d, *J* = 8.4 Hz, 1H), 8.03 (d, *J* = 7.9 Hz, 1H), 7.64 (t, *J* = 7.7 Hz, 1H), 7.22 (t, *J* = 7.7 Hz, 1H). ^{13}C-NMR (101 MHz, DMSO) δ (ppm): 169.41 (s, -COOH), 161.96 (s, oxamaic -COOH), 157.41 (s, -CONH-), 139.96 (s, -PhNH-), 134.64 (s, Ph), 131.84 (s, Ph), 124.16 (s, Ph), 119.98 (s, Ph), 117.55(s, -PhCOOH). FTIR (cm-1): 3213 (w), 1689 (s), 1601 (m), 1586 (m), 1531 (m), 1452 (w), 1375 (m), 1290 (m), 1213 (s), 1190 (s), 1140 (m), 1078 (w), 903 (w), 837 (w), 780 (s), 751 (s), 651(m), 557 (m), 484 (m), 379 (s), 276 (m). Elemental analysis (%): calc. for $C_9H_{7.5}NO_{5.5}Na_{0.5}$. C, 47.17; H, 3.30; N, 6.11 Found: C, 47.95; H, 3.29; N, 6.15.

2.2.3 Synthesis of $[Cu_4Co_3(oaba)_4(OH)_2(DMF)_6]$·2(DMF)·1$H_2O$, (**1**).

$H_{2.5}Na_{0.5}$-oaba·0.5(H_2O) (0.5 mmol, 0.115g) $Cu(OAC)_2.H_2O$ (0.5 mmol, 0.099g), and $Co(OAC)_2.4H_2O$ (0.5 mmol, 0.124 g) were placed in a 23 mL Teflon-lined autoclave reactor filled with DMF (4 mL). The reactor was heated to 80°C in 2 h, kept at this temperature for 72 h and then cooled down to room

temperature in 24 h. Dark purple crystals of **1** were collected and washed by sonication in EtOH. Yield: 0.123 g, 51% (based on copper; M=1889 $gmol^{-1}$). Elemental analysis (%): calc. for $C_{60}H_{76}Co_3Cu_4N_{12}O_{31}$: C, 38.11; H, 4.05; N, 8.89; Co, 9.36; Cu, 13.32 (wt. Cu/Co=1.42). Found: C, 36.97; H, 3.97; N, 8.70; Co, 9,27; Cu, 12,79 (wt. Cu/Co=1.38). Selected IR data (cm^{-1}): 2934(w), 1635(s), 1571(s), 1433(w), 1383(w), 1347(m), 1251(w), 1184(m), 1095(m), 1051(m), 883(w), 852(w), 804(m), 767(m), 716(w), 678(m), 619(w), 580(w), 495(m), 374 (m), 323(m).

2.3. *X-Ray crystallography*

A single crystal of **1** was selected, mounted onto a MiTeGen MiroGripper loop using Paratone-N oil and transferred into a cold nitrogen gas stream produced with an Oxford cooler. Intensity data were collected with a Bruker Kappa-APEXII diffractometer using graphite-monochromated Mo-Kα radiation (λ = 0.71073 Å). Data collection was performed with the Bruker APEXII suite.[38] Unit-cell parameters determination, integration and data reduction were carried out with SAINT program.[38] SADABS was used for scaling and absorption correction.[38,39] The structure was solved with SHELXT-2014,[40] and refined by full-matrix least-squares methods with SHELXL-2014,[41] using the Olex2 software package.[42] It was refined as a 2-component twin (twin law -1 0 1 0 -1 1 0 0 1). All non-hydrogen atoms, except an oxygen atom of a water molecule, were refined anisotropically. The main crystallographic parameters and data refinement results are presented in Table 1. The structure was deposited at the Cambridge Crystallographic Data Centre with number CCDC 1984798 and can be obtained free of charge via www.ccdc.cam.ac.uk/structures.

Table 1. Crystallographic parameters and data refinement for compound **1**.

	1
Formula	$C_{48}H_{46}Co_3Cu_4N_8O_{26}\cdot5(C_3H_7NO),0.3(H_2O)$
FW [g mol^{-1}]	1952.76
Crystal system	Triclinic
Space group	*P-1*
a [Å]	11.192(4)
b [Å]	13.437(5)
c [Å]	15.800(6)
α [°]	111.817(6)
β [°]	105.923(7)
γ [°]	98.564(7)
V [Å^3]	2035.9(13)
Z	1
T [K]	200(2)
λ [Å]	0.71073
ρ_{calc} [g cm^{-3}]	1.593
μ (Mo_{Ka}) [mm^{-1}]	1.709
F(000)	998
Crystal size [mm]	0.3x0.109x0.102
θ limits [°]	1.49-26.79
Measured reflections	26439
Unique reflections	8461
R_{int}	0.0670
R_{sigma}	0.0770
Reflections I>2σ(I)	5710
Parameters	679
Restraints	373
$R_1{}^a$ [I>2σ(I)]	0.1151
$wR_2{}^b$ [I>2σ(I)]	0.2588
GOF	1.093
Largest residuals [eÅ^3]	-1.377;2.386
a: $R_1 = \sum \lVert F_o \rvert - \lvert F_c \rVert / \sum \lvert F_o \rvert$	b: $\omega R_2 = \left[\sum \left(\omega \left(F_o^2 - F_c^2 \right)^2 \right) / \sum \left(\omega \left(F_o^2 \right)^2 \right) \right]^{1/2}$

2.4. Magnetic measurements

Magnetic measurements in dc mode were performed on a polycrystalline sample of **1** restrained within a capsule with a Quantum Design MPMS SQUID. Magnetic susceptibility data were corrected for the diamagnetism of the constituent atoms using the Pascal's constants. The diamagnetism of the sample holder was measured and subtracted from the raw data.

3. Results and discussion

3.1. Synthesis and structure of *1*

The neutral 1D compound **1** (Figure 1) was synthesized solvothermally in DMF at 80 °C with a 1:1:1 stoichiometry (ligand:Cu:Co) and in the lack of base.

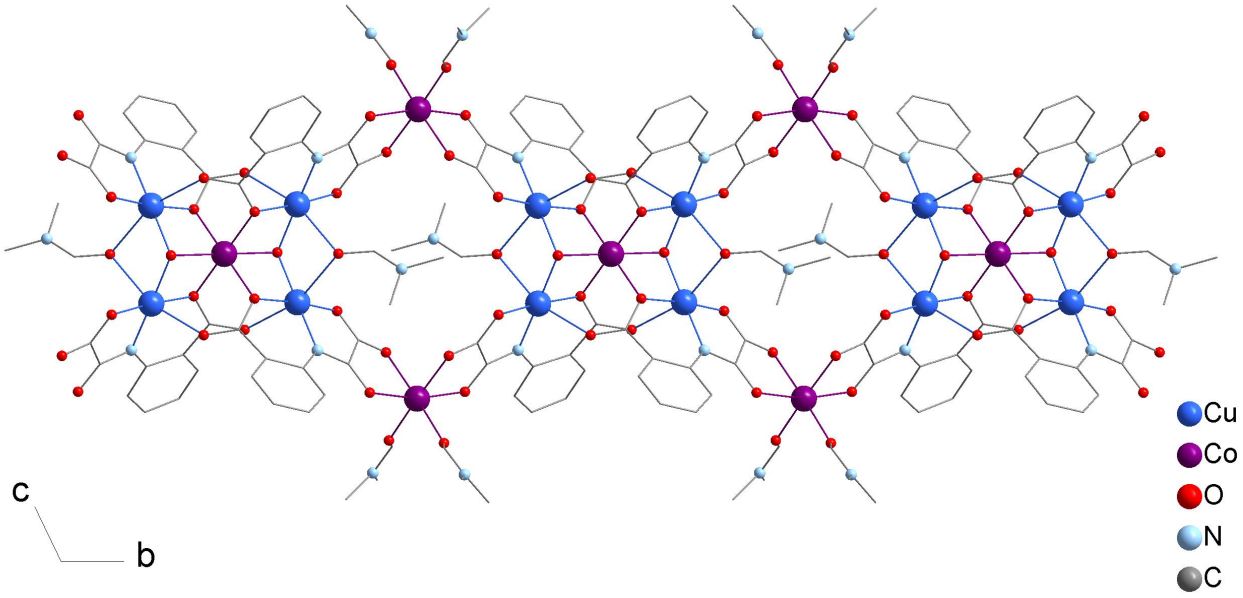

Figure 1. View of the bimetallic chain compound **1**. H atoms and non-coordinated solvent molecules have been omitted for clarity.

The dark purple product crystallizes in the *P*-1 triclinic space group. The asymmetric unit is made of two $(oaba)^{3-}$ ligands, two copper atoms, 1.5 cobalt atoms, one bridging hydroxide ligand, three coordinated DMF molecules and solvents (Figure 2).

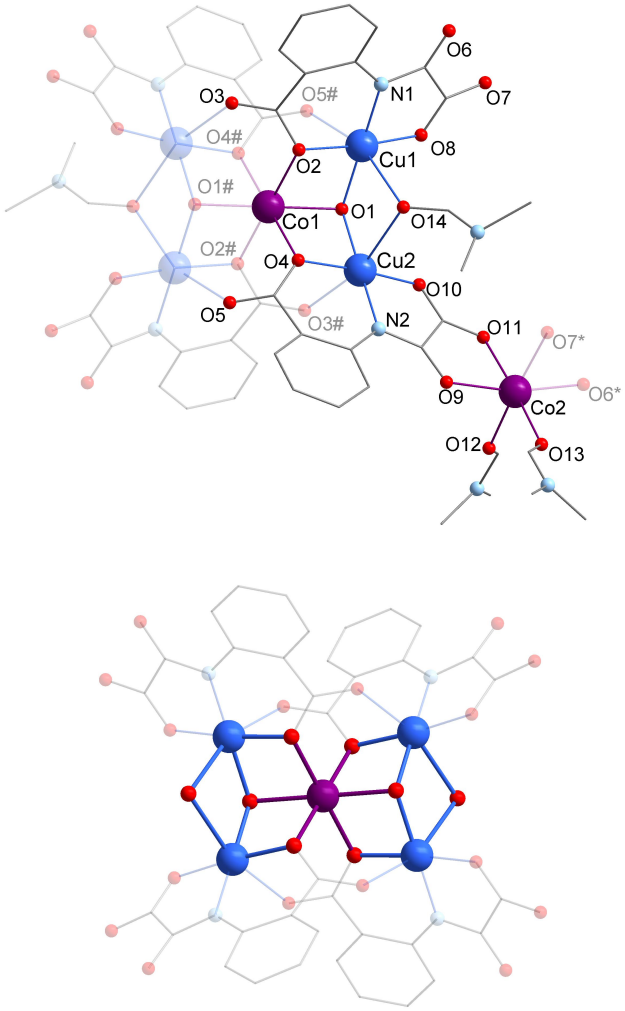

Figure 2. (top) View of the asymmetric unit in the crystal structure of compound **1**. (symmetry codes: #: 1-x,2-y,1-z; *: 1-x,1-y,1-z). (bottom) representation of the lacunar bis-cubane pentametallic core. H atoms and non-coordinated solvent molecules have been omitted for clarity.

Cu1 and Cu2 are structurally identical. Each copper ion is coordinated in a 4+2 geometry. The equatorial plane is partly formed by a tridentate coordination mode of the $(oaba)^{3-}$ ligand using the nitrogen and oxygen atoms of the chelating oxamate group (N1, O8 and N2, O10 for Cu1 and Cu2 respectively) and one oxygen atom of the carboxylate group (O2, O4). The oxygen atom of a μ_3-hydroxide group (O1) that bridges Cu1, Cu2 and Co1 completes the plane. The remaining oxygen atom of the carboxylate group from adjacent $(oaba)^{3-}$ ligands (O5#, O3#), as well as a bridging DMF molecule (O14) complete the coordination spheres of the Cu^{II} ions, resulting in distorted octahedral geometries (O/N_{eq}-Cu-O/N_{eq} from 84 to 97°; O5#-Cu1-O14=161°; O3#-Cu2-O14 = 163°). The Cu-O and Cu-N bond lengths are similar to the previously reported $[Cu\{Cu(oaba)(H_2O)(py)\}_2]$ and $[Cu\{Cu(oaba)(MeOH)\}_2]$ 2D compounds.[25] They range from 1.946(7) to 1.976(7) Å for the equatorial positions and from 2.500(9) to 2.529(5) Å for the apical ones. Co1 and Co2 are both six-coordinate

with an octahedral geometry. Co1 lies on an inversion center and binds the two {Cu(oaba)} metalloligands of the asymmetric unit in a facial manner via the μ_3-hydroxide group (O1) and two carboxylate oxygen atoms (O2, O4). Co2 is *cis*-coordinated to the remaining carbonyl groups of two metalloligands (O6*, O7*, O9 and O11) and has two DMF molecules to complete its coordination sphere. The Co-O distances are quite narrowly distributed, and range from 2.081(6) to 2.135(9) Å. Some distortion is however apparent looking at O-Co-O angles that vary from 78 to 102°, and deviate on average from orthogonality by 6°. Overall, Co1, Cu1 and Cu2 describe a pentametallic sub-unit, $[Co\{Cu(oaba)\}_4(OH)_2(DMF)_2]^{4-}$, that consist of two fused lacunary coordination cubane (Figure 2). This complex then acts as a tetrakis-bidentate ligand and its coordination to Co2 (in a *cis* fashion) generates the 1D arrangement of compound **1** (Figure 3). In comparison to the $[Cu\{Cu(oaba)(H_2O)(py)\}_2]$ and $[Cu\{Cu(oaba)(MeOH)\}_2]$ 2D compounds,[25] the $(oaba)^{3-}$ ligand in **1** binds one extra metal ions, thus acting as a bridge for three metallic pairs, instead of two (Scheme 1). The dimensionality is however lowered, yet the observed morphology contrasts drastically with the linear and zig-zag arrangements commonly observed with phenyloxamate bridging ligands.[11]

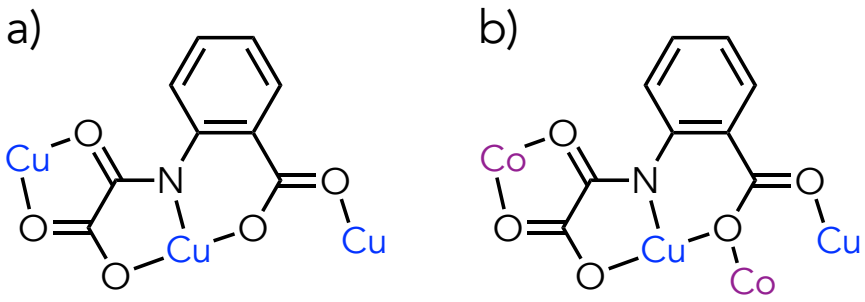

Scheme 1. Representation of the $(oaba)^{3-}$ coordination mode in (a) the $[Cu\{Cu(oaba)(H_2O)(py)\}_2]$ and $[Cu\{Cu(oaba)(MeOH)\}_2]$ 2D compounds,[25] and (b) in compound **1**.

In the crystal, the chain are aligned with each other along the crystallographic *b* axis, and are stacked along *a* (See Supplementary material). There are no obvious supramolecular interactions in the solid. The chains are well isolated within the crystal. The shortest interchain metal-metal distance is between two Co2 atoms and is equal to 8.884(3) Å. Charge balance, BVS calculations and geometric considerations support the presence of Co^{II} and of a hydroxide group. BVS calculations are given as supplementary material.

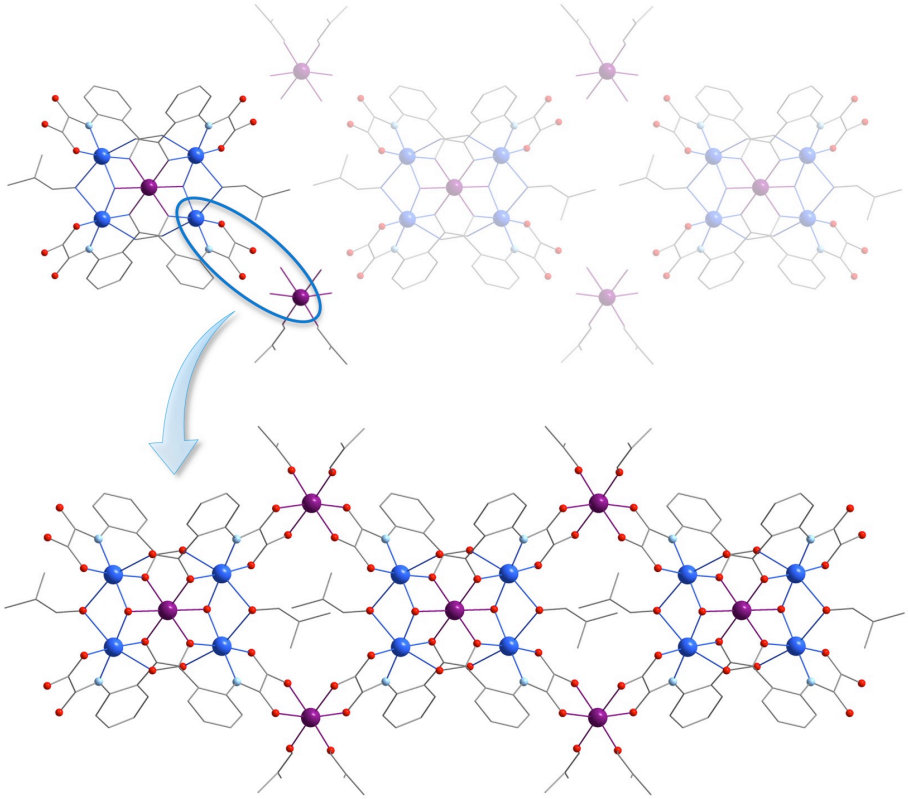

Figure 3. Scheme of the self-assembly in compound **1**. H atoms and non-coordinated solvent molecules have been omitted for clarity.

*3.2. Magnetic properties of **1**.*

The magnetic properties of compound **1** in the form of the $\chi_M T$ *versus* T plot (χ_M is the magnetic susceptibility per $\{Cu_4Co_3\}$ unit) is shown in Figure 4, as well as the magnetic behavior of a hypothetical uncoupled $\{Cu_4Co_3\}$ system. The value of $\chi_M T$ at room temperature is of 9.0 $cm^3mol^{-1}K$, a value which is lower than the smallest value expected for a sum of four Cu^{II} and three Co^{II} non-interacting ions (≈10.1 $cm^3mol^{-1}K$; S_{Cu} = ½ with g = 2.12, $\chi_M T$ (Cu^{II}) = 0.421 $cm^3mol^{-1}K$; octahedral Co^{II} with orbitally degenerate $^4T_{1g}$ ground state, 2.7 < $\chi_M T(Co^{II})$ < 3.4 $cm^3mol^{-1}K$[43]), indicating a strong antiferromagnetic coupling between the ions. Upon cooling, the $\chi_M T$ product steadily decreases down to a value of 2.12 $cm^3mol^{-1}K$ at 2 K. The shape of this curve is typical of the combination of an antiferromagnetic interaction between the magnetic centers with the effect of spin-orbit coupling on the Co^{II} ions. No maximum of χ_M is observed in the temperature range investigated. With a magnetic ordering that cannot be observed *in* a 1D compound,[44] this shows the absence of a magnetic ordering between the well isolated chains in the crystal.

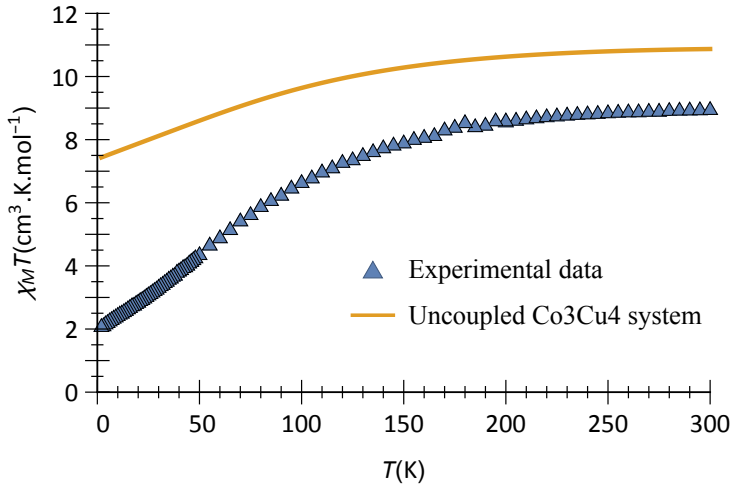

Figure 4. Thermal dependence of $\chi_M T$ for compound **1** in an applied field of 1 T (T ≥ 200K) and 250 Oe (T < 200K). The theoretical curve for an uncoupled $\{Cu_4Co_3\}$ system is calculated taking into account the spin-orbit coupling on the cobalt ions with λ = -180 cm^{-1}, α = 0.9, Δ = -800cm^{-1} (λ, α and Δ being respectively the spin orbit coupling constant, the orbital reduction factor and the distortion parameter), and for copper ions an average *g* factor of 2.12 and a TIP contribution of 60 10^{-6} cm^{3}mol^{-1}.

The *M* versus *H* plot for compound **1** at 2 K (M is the magnetization per $\{Cu_3Co_4\}$ unit and H is the applied magnetic field) is depicted on Figure 5. The observed value of 2.4 Nβ for *M* at 7 T is well below the magnetization saturation value for an uncoupled $\{Co_3Cu_4\}$ system that would reach 10.5 Nβ.

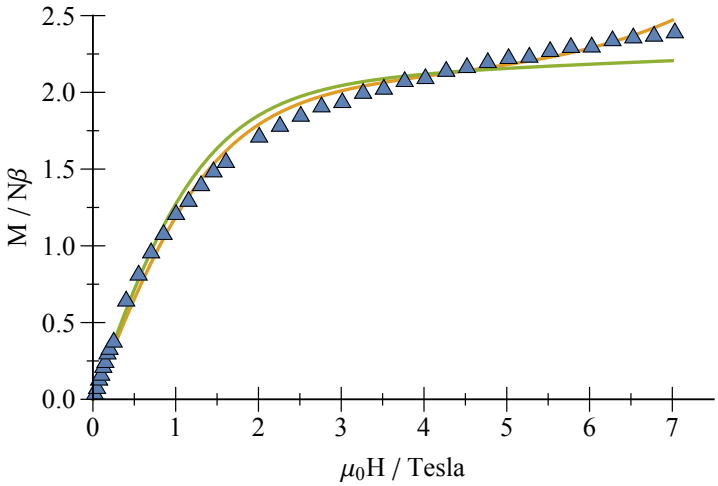

Figure 5. *M v. H* for compound **1** at 2 K (blue triangles). The solid green line represents a fit of *M v. H* taking into account only one Co(II) ion (λ = -130 cm^{-1}, α = 0.82, Δ = 241 cm^{-1}), the orange solid line represents a fit taking into account the $\{Cu_4Co\}$ pentametallic unit (λ = -180 cm^{-1}, α = 0.9, Δ = 42.7 cm^{-1}, J_{CuCu} = -8.7 cm^{-1}, J_{CuCo} = -2.1 cm^{-1})

This confirms the presence of a strong antiferromagnetic coupling between the magnetic ions. The polymeric nature of compound **1** and the composition of the repeating unit that includes four Cu^{II} ions and three Co^{II} ions make it impossible to model the magnetic properties, especially with Co^{II} ions that have first-order orbital momentum. However, the analysis of the structure in correlation with the results published in the literature and the value of 2.4 $N\beta$ found for the magnetization at high field allows us to speculate on the configuration of the spins in the ground state. First, the pentametallic cores bind to Co^{II} ions via oxamato bridges. The interaction between a Co^{II} ion and a Cu^{II} ion across an oxamato bridge is in the -45 to -20 cm^{-1} range.[45,46] Therefore at low temperature the spins of the Co^{II} ions that link the pentametallic units have a direction opposite to that of the neighboring Cu^{II} ions. Within the pentametallic entity, the topology of the interaction is formed by two opposite triangles sharing the central Co^{II} ion as a vertex. If all interactions are antiferromagnetic, this arrangement creates a frustration. The spin configuration will depend on the relative values of the interaction between the Cu^{II} ions and that of the interaction between the Cu^{II} and Co^{II} ions. There are many examples of Cu—Co interaction reported in the literature with either phenoxo[47–54] or alkoxo bridges,[55–60] but very few examples are described with of a μ_3-hydroxo bridge such as in compound **1**.[58,61] Actually, the geometry of the triangle in compound **1** is close to the one observed by Vassilyeva et al,[61] except that the second bridge between the Cu^{II} and Co^{II} ions is not a μ-κO-carboxylato but a μ-alkoxo bridge. Due to its molecular nature and the fact that the Co^{II} ions do not exhibit an orbital moment in their trigonal bipyramid environments, the magnetic properties of Vassilyeva's compound was modeled and all the interactions were found antiferromagnetic. This, along with the analysis of the geometry of the pentametallic entity as well as the other results from the literature, allows us to predict that in compound **1** this should also be the case. The antiferromagnetic interaction is approximately proportional to the square of the overlap of the magnetic orbitals[62] and in the case of monoatomic bridges, such as in compound **1**, the overlap will strongly depend on the angle of the bridge. In particular, this has been well established for hydroxo-bridged Cu(II) ions where the smaller angle, the weaker the coupling.[63–66] For values slightly higher than 90°, the magnetic orbitals are accidentally orthogonal and the coupling is ferromagnetic. In compound **1** the Cu1-O-Cu2 angle is equal to 117.2° and is smaller than that observed in Vassilyeva's compound (119.8°), but it is largely superior than 90°. It excludes ferromagnetic interaction between the two copper ions. The value of the antiferromagnetic Cu—Cu interaction in **1** is therefore probably less than the -86.2 cm^{-1} found in the Vassilyeva's compound but is certainly of one or two tens of wave numbers in absolute value. The geometrical arrangement in **1** also allows a good interaction between the magnetic orbitals of the Co^{II} ion with the magnetic orbital of the Cu^{II} ions. In the literature, {CuCo} compounds with a double bridge consisting of oxygen atoms overwhelming present antiferromagnetic interactions.[67–71] The only examples of ferromagnetic interactions are found when bridges' angles are less than

93°.[72,73] With Cu-O-Co angles comprised between of 95.7 and 97.1°, the coupling is certainly antiferromagnetic as in the reported compounds with angle in the same range.[51,74,75] The two triangles are therefore frustrated, and assumptions must be made to predict the configuration of the spins. If the coupling between the Cu^{II} ions dominates, the spins of the Cu^{II} ions will be antiparallel and so will the spins of the two Co^{II} ions that link the pentametallic units. Under these conditions, the overall behavior should be reminiscent to that of a single Co^{II} ion. The fit of the magnetization curve taking into account only one Co^{II} ion does not give a good result but gives magnetization values that are compatible with the experimental curve (see Figure 5). To go further, the experimental magnetization curve was modeled by taking into account only the pentametallic entity and an acceptable model was obtained. To avoid overparametrization, the spin orbit constant and the orbital reduction factor for the Co^{II} ions were set to standard values (λ = -180cm^{-1}; α = 0.9). The model gives a value for the interaction between the Cu^{II} ions, J_{CuCu} = -8.7 cm^{-1}, that is higher than that between the Cu^{II} ions and the central Co^{II} ion, J_{CuCo} = -2.25 cm^{-1}. In the opposite situation, where the Cu—Co interaction is the strongest, the three spins of the Co^{II} ions will point in the same direction and will be antiparallel to those of the Cu^{II} ions. In this case, the magnetization value at 7 T would be much higher than the observed 2.4 $N\beta$, reaching 5 to 6 $N\beta$, depending on the distortion parameters of the Co^{II} ions (see Figure S3). In light of this analysis, the configuration of the spins at low temperature is dictated by the dominant Cu—Cu interaction, leading to a magnetization behavior reminiscent to that of a single Co^{II} ion.

4. Conclusion

A new heterometallic oxamate-based 1D coordination polymer has been synthesized from a phenyloxamate ligand *ortho*-substituted with a carboxylato group. This compound illustrates the potential of the solvothermal synthetic method to ease the preparation and crystallization of compounds based on complex multi-polydentate oxamate ligands. Indeed, a fully coordinating mode has been observed, thus addressing the deprotonation issues that may occur on the bench with this type of oxamate ligands. The presence of copper ions and its binding affinity for the $\kappa N,\kappa O$ chelating site of the oxamate group undoubtedly facilitate the one-pot solvothermal synthesis of heterometallic compounds. However, if the additional coordinating group successfully yields novel morphologies, even for 1D compounds, it comes at a cost over the predictability of the magnetic interactions and behavior.

Acknowledgements

This work was supported by the Ministère de l'Enseignement Supérieur, de la Recherche et de l'Innovation (MESRI), the Centre National de la Recherche Scientifique (CNRS) and the China

Scholarship Council (CSC) in the form of M. Ang Li's PhD fellowship. Elemental analysis was supported by the IPGP multidisciplinary program PARI, and by Paris–IdF region SESAME Grant no. 12015908. We thank the staff of the low temperature physical measurement MPBT technical platform at Sorbonne Université.

Supplementary material

Supplementary material is available for this article.

References

[1] O. Kahn, Chemistry and Physics of Supramolecular Magnetic Materials, Acc. Chem. Res. 33 (2000) 647–657. https://doi.org/10.1021/ar9703138.

[2] T. Grancha, J. Ferrando-Soria, M. Castellano, M. Julve, J. Pasán, D. Armentano, E. Pardo, Oxamato-based coordination polymers: recent advances in multifunctional magnetic materials, Chem. Commun. 50 (2014) 7569–7585. https://doi.org/10.1039/C4CC01734J.

[3] M. Castellano, R. Ruiz-García, J. Cano, J. Ferrando-Soria, E. Pardo, F.R. Fortea-Pérez, S.-E. Stiriba, W.P. Barros, H.O. Stumpf, L. Cañadillas-Delgado, J. Pasán, C. Ruiz-Pérez, G. de Munno, D. Armentano, Y. Journaux, F. Lloret, M. Julve, Metallosupramolecular approach toward multifunctional magnetic devices for molecular spintronics, Coord. Chem. Rev. 303 (2015) 110–138. https://doi.org/10.1016/j.ccr.2015.05.013.

[4] M. Castellano, R. Ruiz-García, J. Cano, J. Ferrando-Soria, E. Pardo, F.R. Fortea-Pérez, S.-E. Stiriba, M. Julve, F. Lloret, Dicopper(II) Metallacyclophanes as Multifunctional Magnetic Devices: A Joint Experimental and Computational Study, Acc. Chem. Res. 48 (2015) 510–520. https://doi.org/10.1021/ar500378s.

[5] F.R. Fortea-Pérez, M. Mon, J. Ferrando-Soria, M. Boronat, A. Leyva-Pérez, A. Corma, J.M. Herrera, D. Osadchii, J. Gascon, D. Armentano, E. Pardo, The MOF-driven synthesis of supported palladium clusters with catalytic activity for carbene-mediated chemistry, Nat. Mater. 16 (2017) 760–766. https://doi.org/10.1038/nmat4910.

[6] M. Mon, R. Bruno, J. Ferrando-Soria, D. Armentano, E. Pardo, Metal–organic framework technologies for water remediation: towards a sustainable ecosystem, J. Mater. Chem. A. 6 (2018) 4912–4947. https://doi.org/10.1039/C8TA00264A.

[7] M. Viciano-Chumillas, M. Mon, J. Ferrando-Soria, A. Corma, A. Leyva-Pérez, D.

Armentano, E. Pardo, Metal–Organic Frameworks as Chemical Nanoreactors: Synthesis and Stabilization of Catalytically Active Metal Species in Confined Spaces, Acc. Chem. Res. 53 (2020) 520–531. https://doi.org/10.1021/acs.accounts.9b00609.

[8] R. Ruiz, J. Faus, F. Lloret, M. Julve, Y. Journaux, Coordination chemistry of N,N′-bis(coordinating group substituted)oxamides: a rational design of nuclearity tailored polynuclear complexes, Coordination Chemistry Reviews. 193–195 (1999) 1069–1117. https://doi.org/10.1016/S0010-8545(99)00138-1.

[9] E. Pardo, R. Ruiz-Garcia, J. Cano, X. Ottenwaelder, R. Lescouëzec, Y. Journaux, F. Lloret, Miguel. Julve, Ligand design for multidimensional magnetic materials: a metallo-supramolecular perspective., Dalton Trans. (2008) 2780–2805. https://doi.org/10.1039/b801222a.

[10] M.-C. Dul, E. Pardo, R. Lescouëzec, Y. Journaux, J. Ferrando-Soria, R. Ruiz-Garcia, J. Cano, M. Julve, F. Lloret, D. Cangussu, C.L.M. Pereira, H.O. Stumpf, J. Pasan, C. Ruiz-Perez, Supramolecular coordination chemistry of aromatic polyoxalamide ligands: A metallosupramolecular approach toward functional magnetic materials., Coord. Chem. Rev. 254 (2010) 2281–2296. https://doi.org/10.1016/j.ccr.2010.03.003.

[11] Y. Journaux, J. Ferrando-Soria, E. Pardo, R. Ruiz-Garcia, M. Julve, F. Lloret, J. Cano, Y. Li, L. Lisnard, P. Yu, H. Stumpf, C.L.M. Pereira, Design of Magnetic Coordination Polymers Built from Polyoxalamide Ligands: A Thirty Year Story, Eur. J. Inorg. Chem. 2018 (2018) 228–247. https://doi.org/10.1002/ejic.201700984.

[12] T. Grancha, M. Mon, J. Ferrando-Soria, D. Armentano, E. Pardo, Structural Studies on a New Family of Chiral BioMOFs, Crystal Growth & Design. 16 (2016) 5571–5578. https://doi.org/10.1021/acs.cgd.6b01052.

[13] M. Mon, J. Ferrando-Soria, T. Grancha, F.R. Fortea-Pérez, J. Gascon, A. Leyva-Pérez, D. Armentano, E. Pardo, Selective Gold Recovery and Catalysis in a Highly Flexible Methionine-Decorated Metal–Organic Framework, J. Am. Chem. Soc. 138 (2016) 7864–7867. https://doi.org/10.1021/jacs.6b04635.

[14] M. Mon, F. Lloret, J. Ferrando-Soria, C. Martí-Gastaldo, D. Armentano, E. Pardo, Selective and Efficient Removal of Mercury from Aqueous Media with the Highly Flexible Arms of a BioMOF, Angew. Chem. Int. Ed. 55 (2016) 11167–11172. https://doi.org/10.1002/anie.201606015.

[15] T. Grancha, M. Mon, J. Ferrando-Soria, J. Gascon, B. Seoane, E.V. Ramos-Fernandez, D. Armentano, E. Pardo, Tuning the selectivity of light hydrocarbons in natural gas in a family of isoreticular MOFs, J. Mater. Chem. A. 5 (2017) 11032–11039. https://doi.org/10.1039/C7TA01179B.

[16] M. Mon, J. Ferrando-Soria, M. Verdaguer, C. Train, C. Paillard, B. Dkhil, C. Versace, R. Bruno, D. Armentano, E. Pardo, Postsynthetic Approach for the Rational Design of Chiral Ferroelectric Metal–Organic Frameworks, J. Am. Chem. Soc. 139 (2017) 8098–8101. https://doi.org/10.1021/jacs.7b03633.

[17] T. Grancha, X. Qu, M. Julve, J. Ferrando-Soria, D. Armentano, E. Pardo, Rational Synthesis of Chiral Metal–Organic Frameworks from Preformed Rodlike Secondary Building Units, Inorg. Chem. 56 (2017) 6551–6557. https://doi.org/10.1021/acs.inorgchem.7b00681.

[18] T. Grancha, J. Ferrando-Soria, D.M. Proserpio, D. Armentano, E. Pardo, Toward Engineering Chiral Rodlike Metal–Organic Frameworks with Rare Topologies, Inorg. Chem. 57 (2018) 12869–12875. https://doi.org/10.1021/acs.inorgchem.8b02082.

[19] M. Mon, R. Bruno, R. Elliani, A. Tagarelli, X. Qu, S. Chen, J. Ferrando-Soria, D. Armentano, E. Pardo, Lanthanide Discrimination with Hydroxyl-Decorated Flexible Metal–Organic Frameworks, Inorg. Chem. 57 (2018) 13895–13900. https://doi.org/10.1021/acs.inorgchem.8b02409.

[20] M. Mon, R. Bruno, J. Ferrando-Soria, L. Bartella, L.D. Donna, M. Talia, R. Lappano, M. Maggiolini, D. Armentano, E. Pardo, Crystallographic snapshots of host–guest interactions in drugs@metal–organic frameworks: towards mimicking molecular recognition processes, Mater. Horiz. 5 (2018) 683–690. https://doi.org/10.1039/C8MH00302E.

[21] M. Mon, R. Bruno, E. Tiburcio, P.-E. Casteran, J. Ferrando-Soria, D. Armentano, E. Pardo, Efficient Capture of Organic Dyes and Crystallographic Snapshots by a Highly Crystalline Amino-Acid-Derived Metal–Organic Framework, Chem. - Eur. J. 24 (2018) 17712–17718. https://doi.org/10.1002/chem.201803547.

[22] M. Mon, M.A. Rivero-Crespo, J. Ferrando-Soria, A. Vidal-Moya, M. Boronat, A. Leyva-Pérez, A. Corma, J.C. Hernández-Garrido, M. López-Haro, J.J. Calvino, G. Ragazzon, A. Credi, D. Armentano, E. Pardo, Synthesis of Densely Packaged, Ultrasmall Pt02 Clusters within a Thioether-Functionalized MOF: Catalytic Activity in Industrial Reactions at Low Temperature, Angew. Chem. Int. Ed. 57 (2018) 6186–6191.

https://doi.org/10.1002/anie.201801957.

[23] M. Mon, R. Bruno, E. Tiburcio, A. Grau-Atienza, A. Sepúlveda-Escribano, E.V. Ramos-Fernandez, A. Fuoco, E. Esposito, M. Monteleone, J.C. Jansen, J. Cano, J. Ferrando-Soria, D. Armentano, E. Pardo, Efficient Gas Separation and Transport Mechanism in Rare Hemilabile Metal–Organic Framework, Chem. Mater. 31 (2019) 5856–5866. https://doi.org/10.1021/acs.chemmater.9b01995.

[24] C.O. Paul-Roth, Synthesis and characterization of a new bis-oxamide copper(II) complex incorporating a pendant carboxylate function, Comptes Rendus Chimie. 8 (2005) 1232–1236. https://doi.org/10.1016/j.crci.2004.11.007.

[25] K. Yoneda, Y. Hori, M. Ohba, S. Kitagawa, A Homometallic Ferrimagnet Based on Mixed Antiferromagnetic and Ferromagnetic Interactions through Oxamato and Carboxylato Bridges, Chem. Lett. 37 (2008) 64–65. https://doi.org/10.1246/cl.2008.64.

[26] T.L. Oliveira, L.H.G. Kalinke, E.J. Mascarenhas, R. Castro, F.T. Martins, J.R. Sabino, H.O. Stumpf, J. Ferrando, M. Julve, F. Lloret, D. Cangussu, Cobalt(II) and copper(II) assembling through a functionalized oxamate-type ligand, Polyhedron. 81 (2014) 105–114. https://doi.org/10.1016/j.poly.2014.05.051.

[27] T.S. Fernandes, R.S. Vilela, A.K. Valdo, F.T. Martins, E. García-España, M. Inclán, J. Cano, F. Lloret, M. Julve, H.O. Stumpf, D. Cangussu, Dicopper(II) Metallacyclophanes with N,N′-2,6-Pyridinebis(oxamate): Solution Study, Synthesis, Crystal Structures, and Magnetic Properties, Inorg. Chem. 55 (2016) 2390–2401. https://doi.org/10.1021/acs.inorgchem.5b02786.

[28] K. Rühlig, R. Mothes, A. Aliabadi, V. Kataev, B. Büchner, R. Buschbeck, T. Rüffer, H. Lang, CuII bis(oxamato) end-grafted poly(amidoamine) dendrimers, Dalton Trans. 45 (2016) 7960–7979. https://doi.org/10.1039/C5DT03416G.

[29] A. Conte-Daban, V. Borghesani, S. Sayen, E. Guillon, Y. Journaux, G. Gontard, L. Lisnard, C. Hureau, Link between Affinity and Cu(II) Binding Sites to Amyloid-β Peptides Evaluated by a New Water-Soluble UV–Visible Ratiometric Dye with a Moderate Cu(II) Affinity, Anal. Chem. 89 (2017) 2155–2162. https://doi.org/10.1021/acs.analchem.6b04979.

[30] T.S. Fernandes, W.D.C. Melo, L.H.G. Kalinke, R. Rabelo, A.K. Valdo, C.C. da Silva, F.T. Martins, P. Amorós, F. Lloret, M. Julve, D. Cangussu, 2D and 3D mixed MII/CuII metal–organic frameworks (M = Ca and Sr) with N,N′-2,6-pyridinebis(oxamate) and oxalate:

preparation and magneto-structural study, Dalton Trans. 47 (2018) 11539–11553. https://doi.org/10.1039/C8DT01686K.

[31] T.T. da Cunha, V.M.M. Barbosa, W.X.C. Oliveira, C.B. Pinheiro, E.F. Pedroso, W.C. Nunes, C.L.M. Pereira, Slow magnetic relaxation in mononuclear gadolinium(III) and dysprosium(III) oxamato complexes, Polyhedron. 169 (2019) 102–113. https://doi.org/10.1016/j.poly.2019.04.056.

[32] L. Hou, L.-N. Ma, X.-Y. Li, Y.-Z. Li, W.-J. Shi, G. Liu, Y.-Y. Wang, Structural Diversity of CPs Induced by Coordinating Modes of a New Bis(oxamate) Ligand: Luminescent and Magnetic Properties, ChemPlusChem. 84 (2019) 62–68. https://doi.org/10.1002/cplu.201800470.

[33] J. Maciel, L. Kalinke, A. Valdo, F. Martins, R. Rabelo, N. Moliner, J. Cano, M. Julve, F. Lloret, D. Cangussu, New Metal-Organic Systems with a Functionalized Oxamate-Type Ligand and MnII, FeII, CuII and ZnII, J. Braz. Chem. Soc. 30 (2019) 2413–2429. https://doi.org/10.21577/0103-5053.20190158.

[34] A. Li, Y. Li, L.-M. Chamoreau, C. Desmarets, L. Lisnard, Y. Journaux, A Bis-Polydentate Oxamate-Based Achiral Ligand That Can Stabilize a Macrocyclic Mixed Valence Compound or Induce a 1D Helical Chain, Eur. J. Inorg. Chem. 2020 (2020) 3311–3319. https://doi.org/10.1002/ejic.202000490.

[35] L. Lisnard, L.-M. Chamoreau, Y. Li, Yves. Journaux, Solvothermal Synthesis of Oxamate-Based Helicate: Temperature Dependence of the Hydrogen Bond Structuring in the Solid., Cryst. Growth Des. 12 (2012) 4955–4962. https://doi.org/10.1021/cg300877r.

[36] A. Li, L.-M. Chamoreau, B. Baptiste, Y. Li, Y. Journaux, L. Lisnard, Solvothermal synthesis, structure and magnetic properties of heterometallic coordination polymers based on a phenolato-oxamato co-bidentate-tridentate ligand, Dalton Trans. (2020). https://doi.org/10.1039/D0DT03269G.

[37] B. Cervera, J.L. Sanz, M.J. Ibáñez, G. Vila, F. LLoret, M. Julve, R. Ruiz, X. Ottenwaelder, A. Aukauloo, S. Poussereau, Y. Journaux, M.C. Munoz, Stabilization of copper (III) complexes by substituted oxamate ligands, J. Chem. Soc., Dalton Trans. (1998) 781–790. https://doi.org/10.1039/A706964B.

[38] BrukerAXS Inc, Madison, Wisconsin, USA, 1998.

[39] R.H. Blessing, An empirical correction for absorption anisotropy, Acta Cryst A. 51

(1995) 33. https://doi.org/10.1107/S0108767394005726.

[40] G.M. Sheldrick, SHELXT – Integrated space-group and crystal-structure determination, Acta Cryst A. 71 (2015) 3–8. https://doi.org/10.1107/S2053273314026370.

[41] G.M. Sheldrick, Crystal structure refinement with SHELXL, Acta Crystallogr., Sect. C. 71 (2015) 3–8. https://doi.org/10.1107/S2053229614024218.

[42] O.V. Dolomanov, L.J. Bourhis, R.J. Gildea, J. a. K. Howard, H. Puschmann, OLEX2: a complete structure solution, refinement and analysis program, J Appl Cryst. 42 (2009) 339–341. https://doi.org/10.1107/S0021889808042726.

[43] F. Lloret, M. Julve, J. Cano, R. Ruiz-Garcia, Emilio. Pardo, Magnetic properties of six-coordinated high-spin cobalt(II) complexes: Theoretical background and its application., Inorg. Chim. Acta. 361 (2008) 3432–3445. https://doi.org/10.1016/j.ica.2008.03.114.

[44] F. Palacio, From Ferromagnetic Interactions to Molecular Ferromagnets : An Overview of Models and Materials, in: Magnetic Molecular Materials, Kluwer Academic Publishers, D. Gatteschi, O. Kahn, J. Miller, F. Palacio, Dordrecht Boston London, 1991: pp. 1–34.

[45] P.J. Van Koningsbruggen, O. Kahn, K. Nakatani, Y. Pei, J.P. Renard, M. Drillon, P. Legoll, Magnetism of A-copper(II) bimetallic chain compounds (A = iron, cobalt, nickel): one- and three-dimensional behaviors, Inorg. Chem. 29 (1990) 3325–3331. https://doi.org/10.1021/ic00343a014.

[46] E. Pardo, R. Ruiz-Garcia, F. Lloret, J. Faus, M. Julve, Y. Journaux, M.A. Novak, F.S. Delgado, Catalina. Ruiz-Perez, Ligand design for heterobimetallic single-chain magnets: synthesis, crystal structures, and magnetic properties of MIICuII (M = Mn, Co) chains with sterically hindered methyl-substituted phenyloxamate bridging ligands., Chem. Eur. J. 13 (2007) 2054–2066, S2054/1-S2054/5. https://doi.org/10.1002/chem.200600992.

[47] C.J. O'Connor, D.P. Freyberg, E. Sinn, Relation between structure and magnetic exchange interactions in bis(hexafluoroacetylacetonato){N,N'-ethylenebis[2-hydroxypropiophenone iminato-N,O(2-)]copper(II)}M'(II), Cu((prp)2en)M'(hfa)2, where M' = Cu, Ni, and Mn. Crystal structures of the complexes(M((prp)2en)M'(hfa)2), Inorg. Chem. 18 (1979) 1077–1088. https://doi.org/10.1021/ic50194a038.

[48] M. Mikuriya, H. Okawa, S. Kida, I. Ueda, Binuclear Metal Complexes, XXIII. Molecular Structure of a Heterometal Binuclear Complex, CuCo(fsaen)·3H2O(C18H18N2O9CoCu), Bull. Chem. Soc. Jpn. 51 (1978) 2920–2923. https://doi.org/10.1246/bcsj.51.2920.

[49] J. Galy, J. Jaud, O. Kahn, P. Tola, Crystal and molecular structure of CuCo(fsa)2en.6H2O(H4(fsa)2en = N,N'-bis(2-hydroxy-3-carboxybenzylidene)-1,2-diaminoethane): an example of close-packed association of two heterobinuclear units through the formation of a water molecule network, Inorg. Chem. 19 (1980) 2945–2948. https://doi.org/10.1021/ic50212a021.

[50] D.G. Branzea, A.M. Madalan, S. Ciattini, N. Avarvari, A. Caneschi, M. Andruh, New heterometallic coordination polymers constructed from 3d–3d′ binuclear nodes, New J. Chem. 34 (2010) 2479–2490. https://doi.org/10.1039/C0NJ00238K.

[51] S. Ghosh, G. Aromí, P. Gamez, A. Ghosh, The Impact of Anion-Modulated Structural Variations on the Magnetic Coupling in Trinuclear Heterometallic CuII–CoII Complexes Derived from a Salen-Type Schiff Base Ligand, European Journal of Inorganic Chemistry. 2014 (2014) 3341–3349. https://doi.org/10.1002/ejic.201402151.

[52] S. Ghosh, G. Aromi, P. Gamez, A. Ghosh, Structural and Magnetic Analysis of Retrosynthetically Designed Architectures Built from a Triply Bridged Heterometallic (CuL)2Co Node and Benzenedicarboxylates, European Journal of Inorganic Chemistry. 2015 (2015) 3028–3037. https://doi.org/10.1002/ejic.201500273.

[53] C.N. Verani, E. Rentschler, T. Weyhermüller, E. Bill, P. Chaudhuri, Exchange coupling in a bis(heterodinuclear) [CuIINiII]2 and a linear heterotrinuclear complex CoIIICuIINiII. Synthesis, structures and properties, J. Chem. Soc., Dalton Trans. (2000) 251–258. https://doi.org/10.1039/A908426F.

[54] N. Hari, S. Mandal, A. Jana, H.A. Sparkes, S. Mohanta, Syntheses, crystal structures, magnetic properties and ESI-MS studies of a series of trinuclear CuIIMIICuII compounds (M = Cu, Ni, Co, Fe, Mn, Zn), RSC Adv. 8 (2018) 7315–7329. https://doi.org/10.1039/C7RA13763J.

[55] E. Martin, V. Tudor, A.M. Madalan, C. Maxim, F. Tuna, F. Lloret, M. Julve, M. Andruh, Heterometallic CoII-CoIII-MII alkoxido-bridged heptanuclear motifs (M=Cu, Zn). Syntheses, crystal structures and magnetic properties, Inorganica Chimica Acta. 475 (2018) 98–104. https://doi.org/10.1016/j.ica.2017.05.077.

[56] D.S. Nesterov, V.N. Kokozay, V.V. Dyakonenko, O.V. Shishkin, J. Jezierska, A. Ozarowski, A.M. Kirillov, M.N. Kopylovich, A.J.L. Pombeiro, An unprecedented heterotrimetallic Fe/Cu/Co core for mild and highly efficient catalytic oxidation of cycloalkanes

by hydrogen peroxide, Chem. Commun. (2006) 4605–4607. https://doi.org/10.1039/B608790F.

[57] D.S. Nesterov, V.G. Makhankova, O.Yu. Vassilyeva, V.N. Kokozay, L.A. Kovbasyuk, B.W. Skelton, J. Jezierska, Assembling Novel Heterotrimetallic Cu/Co/Ni and Cu/Co/Cd Cores Supported by Diethanolamine Ligand in One-Pot Reactions of Zerovalent Copper with Metal Salts, Inorg. Chem. 43 (2004) 7868–7876. https://doi.org/10.1021/ic048955w.

[58] M. Hamid, A.A. Tahir, M. Mazhar, M. Zeller, K.C. Molloy, A.D. Hunter, Synthesis of Isostructural Cage Complexes of Copper with Cobalt and Nickel for Deposition of Mixed Ceramic Oxide Materials, Inorg. Chem. 45 (2006) 10457–10466. https://doi.org/10.1021/ic060119u.

[59] T. Nakajima, C. Yamashiro, M. Taya, B. Kure, T. Tanase, Systematic Synthesis of Di-, Tri-, and Tetranuclear Homo- and Heterometal Complexes Using a Mononuclear Copper Synthon with a Tetradentate Amino Alcohol Ligand, European Journal of Inorganic Chemistry. 2016 (2016) 2764–2773. https://doi.org/10.1002/ejic.201600142.

[60] M. Sultan, A.A. Tahir, M. Mazhar, M. Zeller, K.G.U. Wijayantha, Hexanuclear copper–nickel and copper–cobalt complexes for thin film deposition of ceramic oxide composites, New J. Chem. 36 (2012) 911–917. https://doi.org/10.1039/C2NJ20789C.

[61] V.G. Makhankova, O.Y. Vassilyeva, V.N. Kokozay, B.W. Skelton, L. Sorace, D. Gatteschi, Novel polynuclear CuII/CoII complexes constructed from one and two Cu2Co triangles with antiferromagnetic exchange coupling, J. Chem. Soc., Dalton Trans. (2002) 4253–4259. https://doi.org/10.1039/B205389F.

[62] O. Kahn, Molecular Magnetism, VCH Publishers Inc, New York, 1993.

[63] V.H. Crawford, H.Wayne. Richardson, J.R. Wasson, D.J. Hodgson, W.E. Hatfield, Relation between the singlet-triplet splitting and the copper-oxygen-copper bridge angle in hydroxo-bridged copper dimers, Inorg. Chem. 15 (1976) 2107–2110. https://doi.org/10.1021/ic50163a019.

[64] P.J. Hay, J.C. Thibeault, R. Hoffmann, Orbital interactions in metal dimer complexes, J. Am. Chem. Soc. 97 (1975) 4884–4899. https://doi.org/10.1021/ja00850a018.

[65] E. Ruiz, P. Alemany, S. Alvarez, J. Cano, Toward the Prediction of Magnetic Coupling in Molecular Systems: Hydroxo- and Alkoxo-Bridged Cu(II) Binuclear Complexes, J. Am. Chem. Soc. 119 (1997) 1297–1303. https://doi.org/10.1021/ja961199b.

[66] E. Ruiz, P. Alemany, S. Alvarez, J. Cano, Structural Modeling and Magneto–Structural Correlations for Hydroxo-Bridged Copper(II) Binuclear Complexes, Inorg. Chem. 36 (1997) 3683–3688. https://doi.org/10.1021/ic970310r.

[67] T. Aono, H. Wada, M. Yonemura, H. Furutachi, M. Ohba, H. Okawa, Diphenoxo-bridged NiCo and CuCo complexes of macrocyclic ligands:synthesis, structure and electrochemical behaviour, J. Chem. Soc., Dalton Trans. (1997) 3029–3034. https://doi.org/10.1039/A702210G.

[68] M. Nayak, R. Koner, H.-H. Lin, U. Flörke, H.-H. Wei, S. Mohanta, Syntheses, Structures, and Magnetic Properties of Mononuclear CuII and Tetranuclear CuII3MII (M = Cu, Co, or Mn) Compounds Derived from N,N‘-Ethylenebis(3-ethoxysalicylaldimine): Cocrystallization Due to Potential Encapsulation of Water, Inorg. Chem. 45 (2006) 10764–10773. https://doi.org/10.1021/ic061049u.

[69] R.-J. Tao, C.-Z. Mei, S.-Q. Zang, Q.-L. Wang, J.-Y. Niu, D.-Z. Liao, Synthesis, characterization, crystal structures and magnetic properties of dissymmetrical double schiff base heterotrinuclear complexes: [CuL(H2O)CoCuL]·H2O·CH3OH and [(CuL)2Ni]·2H2O, Inorganica Chimica Acta. 357 (2004) 1985–1990. https://doi.org/10.1016/j.ica.2003.12.032.

[70] Y. Sunatsuki, T. Matsuo, M. Nakamura, F. Kai, N. Matsumoto, J.-P. Tuchagues, Synthesis, Structure, and Properties of Di-μ-phenoxo-bridged Dinuclear CuIINiII and CuIICoII Complexes and Cyclic Di-μ-phenoxo-μ-amido-bridged Tetranuclear Cu2IIZn2II and Cu4IIComplexes Derived from the 1,2-Bis(2-oxidobenzamidato)benzenecuprate(II) Dianionic Ligand-Complex, BCSJ. 71 (1998) 2611–2619. https://doi.org/10.1246/bcsj.71.2611.

[71] M. Yonemura, K. Arimura, K. Inoue, N. Usuki, M. Ohba, H. Okawa, Coordination-Position Isomeric MIICuII and CuIIMII (M = Co, Ni, Zn) Complexes Derived from Macrocyclic Compartmental Ligands, Inorg. Chem. 41 (2002) 582–589. https://doi.org/10.1021/ic010499d.

[72] D.S. Nesterov, V.N. Kokozay, B.W. Skelton, J. Jezierska, A. Ozarowski, Self-assembly of the unique heterotrimetallic Cu/Co/M complexes possessing triangular antiferromagnetic {Cu2CoPb}2 and linear ferromagnetic {Cu2CoCd2} cores, Dalton Trans. (2007) 558–564. https://doi.org/10.1039/B612788F.

[73] K. Matsumoto, N. Sekine, K. Arimura, M. Ohba, H. Sakiyama, H. Okawa, μ-Acetato-di-μ-phenolato-metal(II)cobalt(II) (Metal = Fe, Co, Ni, Cu, Zn) Complexes with Low-Spin Co(II):

Synthesis, Structures, and Magnetism, Bull. Chem. Soc. Jpn. 77 (2004) 1343–1351. https://doi.org/10.1246/bcsj.77.1343.

[74] S. Ghosh, S. Giri, A. Ghosh, An adaptable heterometallic trinuclear coordination cluster in the synthesis of tailored one-dimensional architecture: Structural characterization, magnetic analysis and theoretical calculations, Polyhedron. 102 (2015) 366–374. https://doi.org/10.1016/j.poly.2015.10.014.

[75] J. Parreiras, E.N. Faria, W.X.C. Oliveira, W.D.D. Pim, R.V. Mambrini, E.F. Pedroso, M. Julve, C.L.M. Pereira, H.O. Stumpf, Solvent effects on the dimensionality of oxamato-bridged manganese(II) compounds, J. Coord. Chem. 71 (2018) 797–812. https://doi.org/10.1080/00958972.2018.1439162.

Supplementary Material for:

Synthesis, structure and magnetic properties of an oxamate-based 1D coordination polymer built on pentametallic links.

Ang Li (李昂),[a] Jérémy Forté,[a] Yanling Li,[a] Laurent Lisnard,*[a] Yves Journaux*[a]

a. Sorbonne Université, CNRS, Institut Parisien de Chimie Moléculaire, IPCM, F-75252, Paris, France.

*Corresponding author: laurent.lisnard@sorbonne-universite.fr

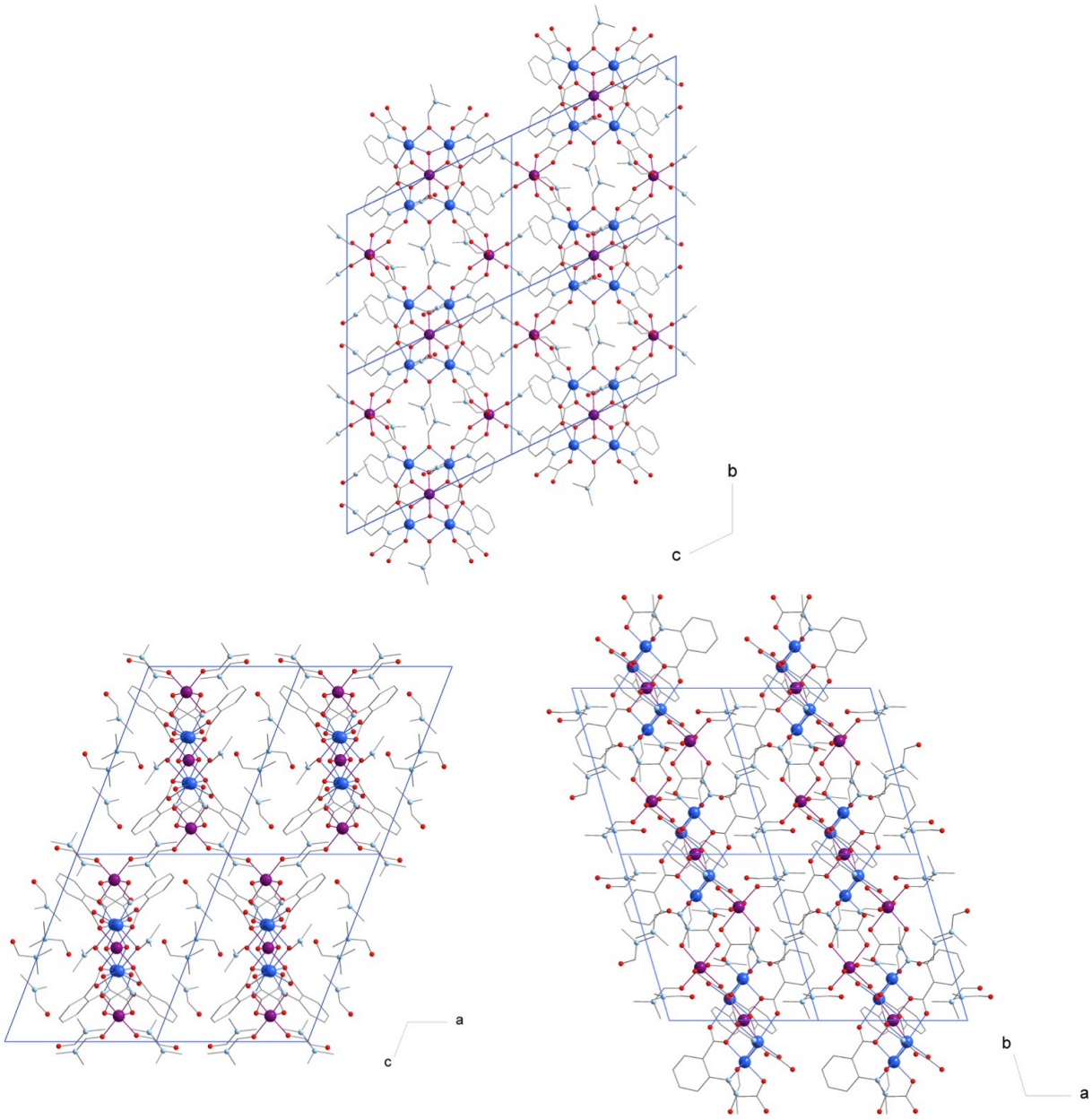

Figure S1. Crystal packing for **1**.

Atoms	dist.	Co(II)	Co(III)	Atoms	dist.	Co(II)	Co(III)
Co1 O4	2.0893	0.342	0.349	Co2 O13	2.081	0.349	0.357
O4	2.0896	0.341	0.349	O9	2.0815	0.349	0.357
O1	2.0929	0.338	0.346	O6	2.0875	0.343	0.351
O1	2.0936	0.338	0.345	O12	2.0875	0.343	0.351
O2	2.1038	0.328	0.336	O11	2.1136	0.32	0.327
O2	2.1049	0.328	0.335	O7	2.1347	0.302	0.309
		2.016	2.056			2.007	2.051

Table S1. BVS calculations.[*N.E. Brese, M. O'Keeffe, Acta Crystallogr., Sect. B. 47 (1991) 192–197; M. O'Keeffe, N.E. Brese, Acta Crystallogr., Sect. B. 48 (1992) 152–154.*]

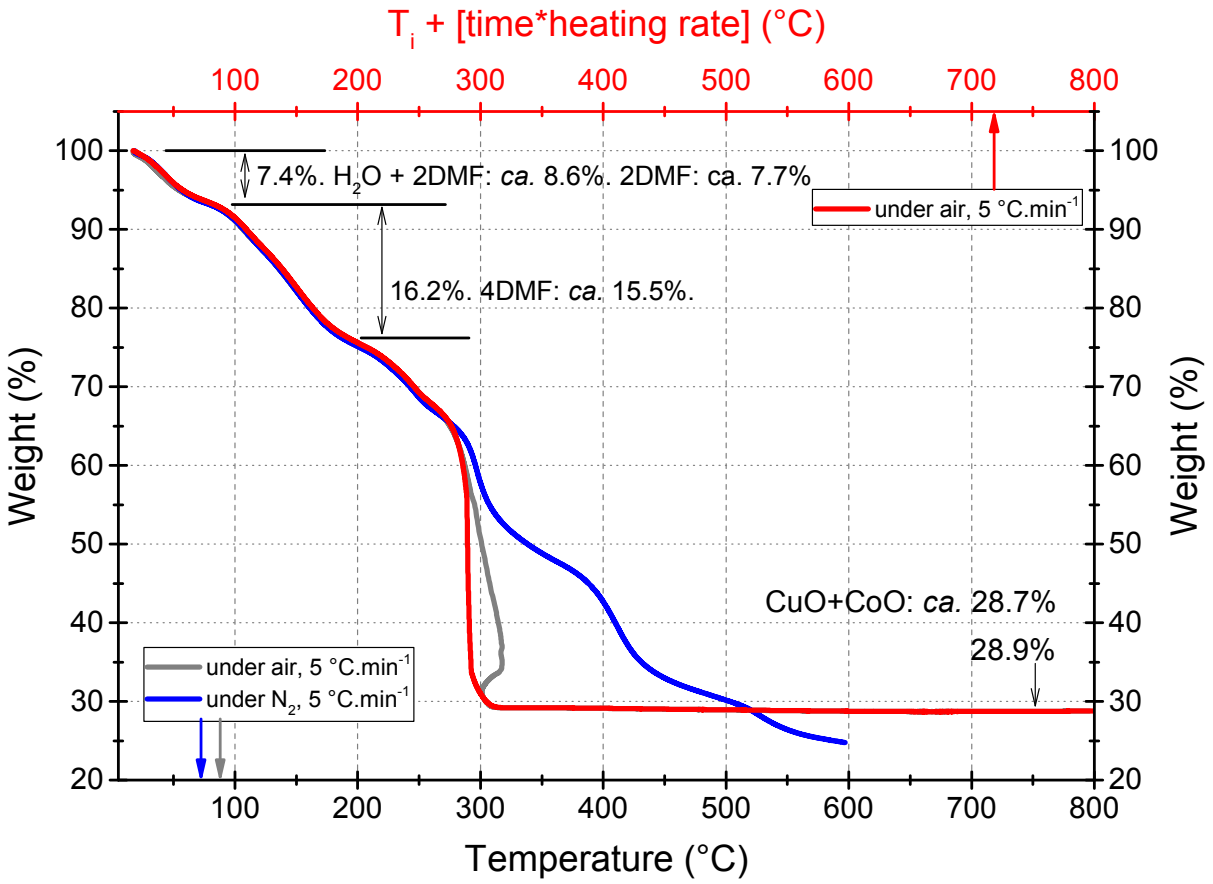

Figure S2. TGA of compound **1**, under air and under N_2 at a rate of 5 °C/min. Due to a combustion phenomenon, data under air are also given using experiment duration times heating rate as a scale (upper one, in red).

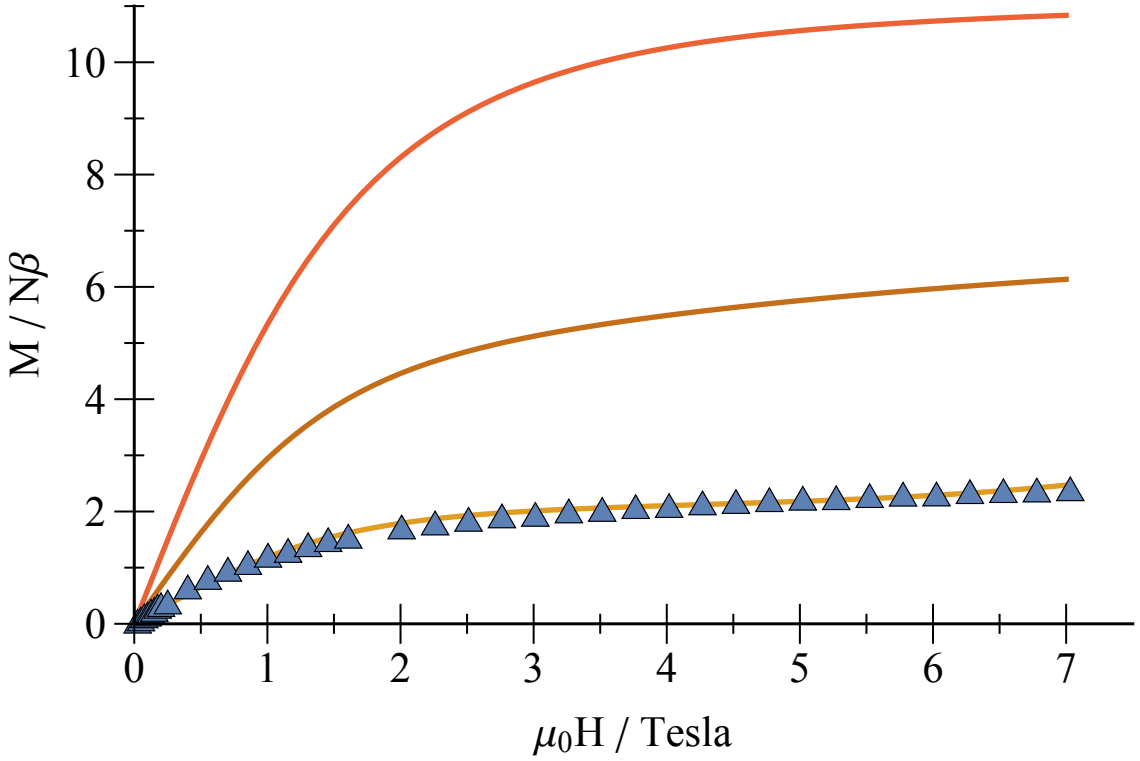

Figure S3. Magnetization of compound **1** versus magnetic field at 2 K. The orange solid line represents a fit taking into account the $\{Cu_4Co\}$ pentametallic unit (λ = -180 cm^{-1} –fixed; α = 0.9 -fixed; Δ = 42.7 cm^{-1}, J_{CuCu} = -8.7cm^{-1}, J_{CuCo} = -2.1cm^{-1}), The brown solid line represents a simulation of the spin configuration where J_{CuCo} is the dominant interaction leading to the spin configuration where all the spins of the Cu^{II} ions have the same direction antiparallel to those of the three Co^{II} ions (λ = -180 cm^{-1}, α = 0.9, Δ = 40 cm^{-1}, J_{CuCo} = -50 cm^{-1}, J_{CuCu} = -5 cm^{-1}, g_{Cu}=2.15). The red solid line represents a simulation for the magnetization of an hypothetical $\{Cu_4Co_3\}$ uncoupled system (λ = -180 cm^{-1}, α = 0.9, Δ = 40 cm^{-1}, g_{Cu} = 2.15).